Supplementary Information for:

A supramolecular chain of dimeric Dy single-molecule magnets decorated with azobenzene ligands

Gang Huang,[a] Xiaohui Yi,[a] Frederic Gendron,[a] Boris le Guennic,[a] T. Guizouarn,[a] Carole Daiguebonne,[a] Guillaume Calvez,[a] Yan Suffren,[a] Olivier Guillou[a] and Kevin Bernot[a]

[a]Univ Rennes, INSA Rennes, CNRS, ISCR (Institut des Sciences Chimiques de Rennes), UMR 6226, F-35000 Rennes, France.

Table S1. Main crystallographic parameters for **DyAZO**.

Formula	$C_{90}\ H_{58}\ Dy_2\ N_{12}\ O_{20}\ S_6$
M [g.mol^{-1}]	2181.13
Crystal system	triclinic
Space group	*P*-1 (N°2)
a (Å)	8.2837(5)
b (Å)	16.9284(11)
c (Å)	18.0074(12)
α [°]	73.133(2)
β [°]	82.367(2)
γ [°]	86.299(2)
V [Å^3]	2394.2(3)
Z	1
T(K)	298
2θ range	2.35-27.47
Reflns collected	9949
Independent reflns	10936
Observed reflns	9919
Parameters	594
$R1/\omega R^2$	0.0282/0.0887
Goof	1.054

Table S2. Selected bond lengths and angles for **DyAZO**.

Bond	Distance (Å)	Atoms	Angle (°)
Dy1-O1	2.3413(18)	O2-Dy1-O6	53.79(6)
Dy1-O2	2.4782(18)	O5-Dy1-O7	53.30(5)
Dy1-O3	2.3580(19)	O1-Dy1-O4	77.49(7)
Dy1-O4	2.2800(19)	O3-Dy1-O2	149.80(6)
Dy1-O5	2.4090(18)	O8-Dy1-O3	77.58(7)
Dy1-O6	2.381(2)	O1-Dy1-O7	145.43(6)
Dy1-O7	2.4842(19)	O2-Dy1-O7	123.55(6)
Dy1-O8	2.2731(18)	O8-Dy1-O6	73.39(6)

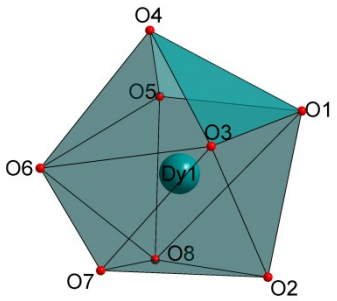

Figure S1. Coordination polyhedron of Dy1 in **DyAZO**.

Table S3. Continuous Shape Measurements (CShM) on Dy1 in **DyAZO**.

Coordination geometry (site symmetry)	Square antiprism (D_{4d})	Bi-augmented trigonal prism (C_{2v})
CShM	3.074	2.374

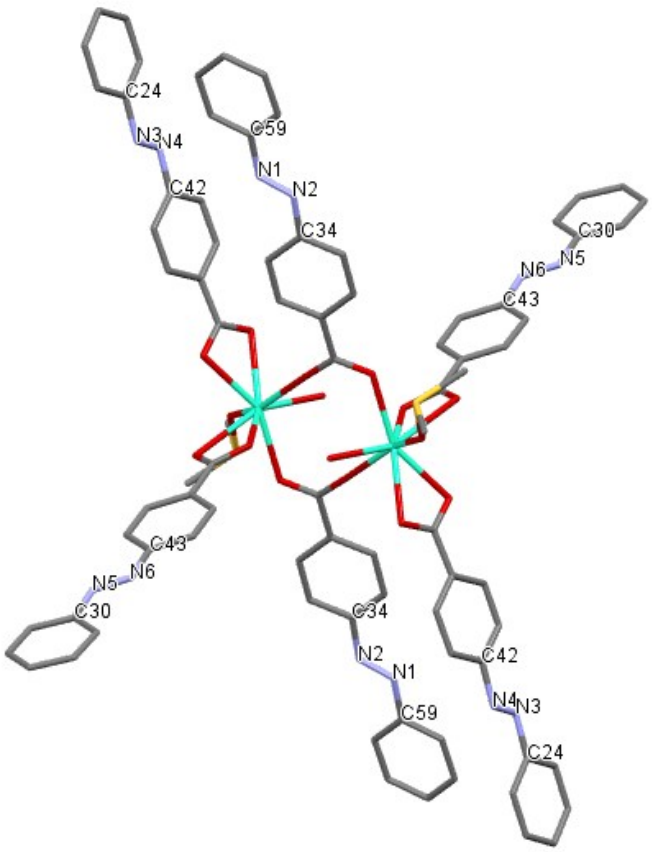

Figure S2: Representation of **DyAZO** with labelling scheme on the azobenzene nitrogen atoms

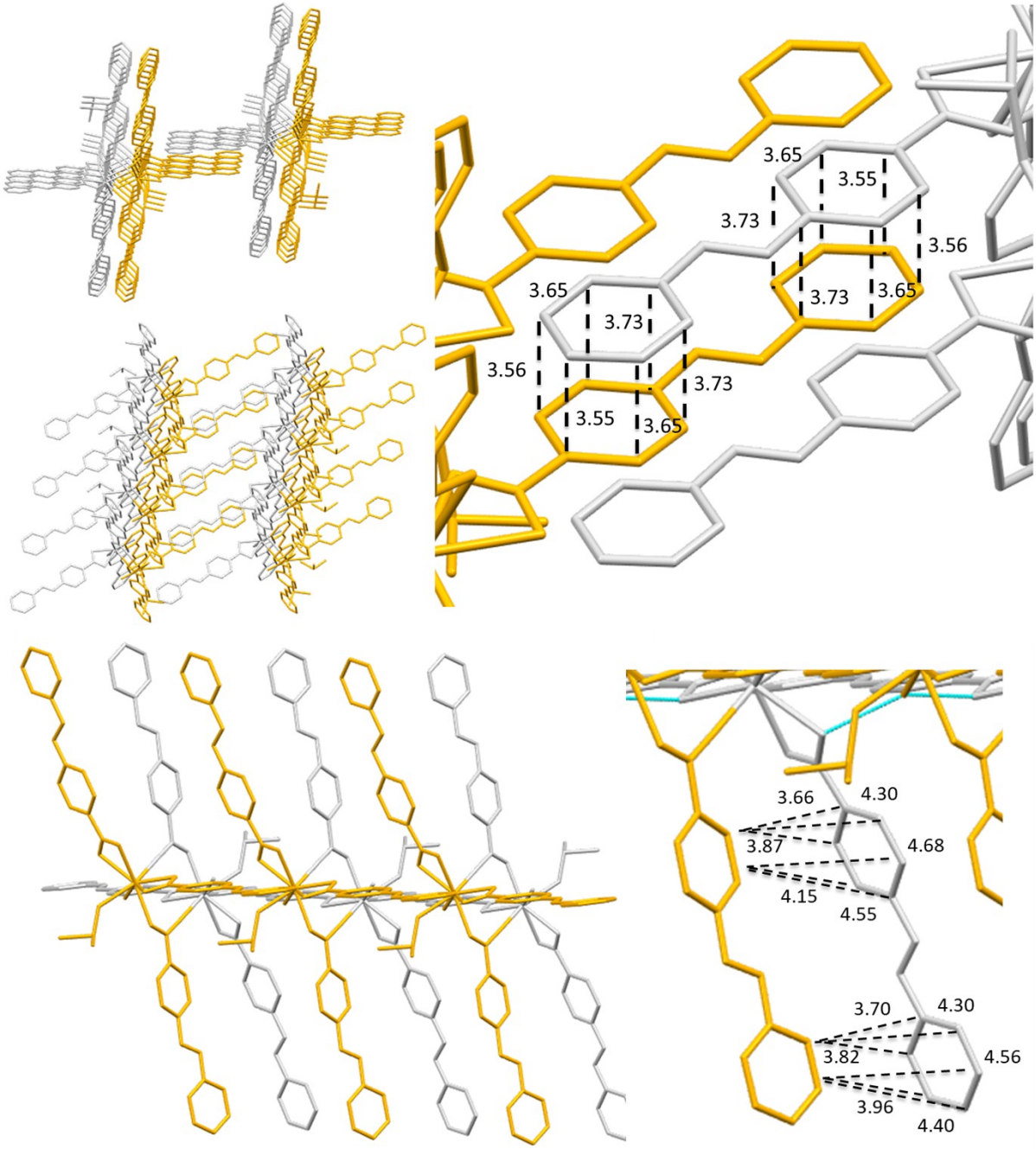

Figure S3: Representation of the intermolecular stacking interaction in **DyAZO** with distances between carbon atoms (Bottom)

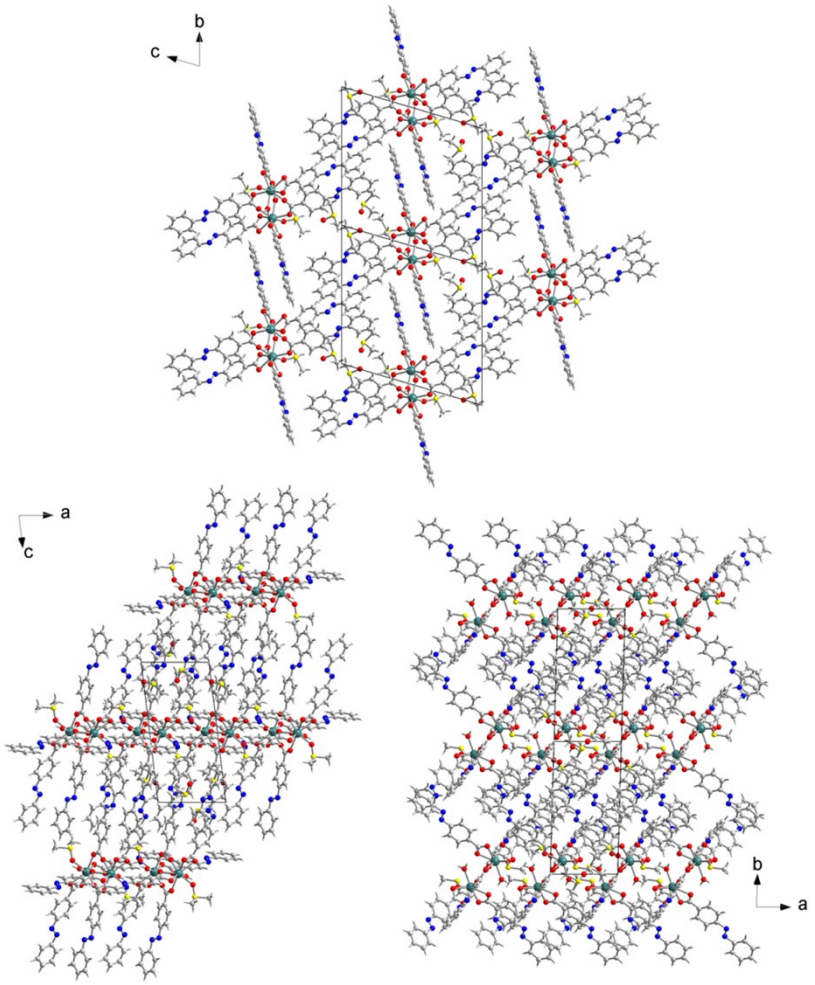

Figure S4. Crystal packing views of **DyAZO.**

Table S4. Calculated relative energies (ΔE in cm^{-1}) and EPR g-factors for the Kramers doublets deriving from the $^6H_{15/2}$ level of the two Dy^{3+} ions in the model compound.

	Center1				Center2			
	ΔE	g1	g2	g3	ΔE	g1	g2	g3
GS	0	0.445	0.468	17.278	0	0.447	0.470	17.297
ES1	34	0.911	3.699	14.583	34	0.918	3.704	14.590
ES2	47	1.317	3.510	11.516	47	1.315	3.521	11.518
ES3	97	1.207	2.422	14.112	97	1.215	2.434	14.097
ES4	135	1.192	4.516	8.880	135	1.213	4.549	8.853
ES5	155	3.771	5.231	11.443	155	3.764	5.178	11.471
ES6	185	0.037	0.554	18.190	185	0.033	0.559	18.179
ES7	402	0.000	0.001	19.739	402	0.000	0.001	19.738

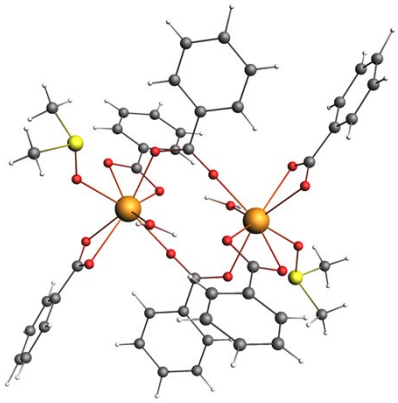

Figure S5. Molecular representation of the **DyAZO** model compound used for WFT calculations.

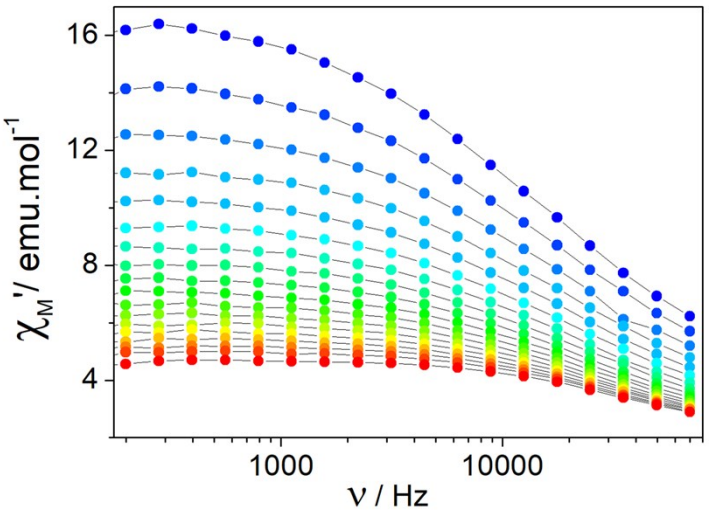

Figure S6. Frequency dependence of the in-phase component of the magnetization measured on **DyAZO** with $\mathbf{H_{dc}}$ **= 0 Oe** between 1.6 K (blue) and 7.6 K (red) (0.2 K spacing).

Table S5. Relaxation times extracted for **DyAZO** with $\mathbf{H_{dc}}$ **= 0 Oe**.

T (K)	τ (μs)	T (K)	τ (μs)
1.56	12.08	3.6	7.41
1.6	11.71	3.8	7.27
1.7	11.65	4	7.14
1.8	11.00	4.2	6.63
1.9	10.62	4.4	7.28
2	10.67	4.6	6.08
2.1	10.05	4.8	5.79
2.2	9.94	5	5.73
2.3	9.87		
2.4	9.52		
2.5	9.7		
2.6	10.26		
2.7	9.15		
2.8	9.24		
2.9	8.7		
3	8.49		
3.2	8.50		
3.4	7.98		

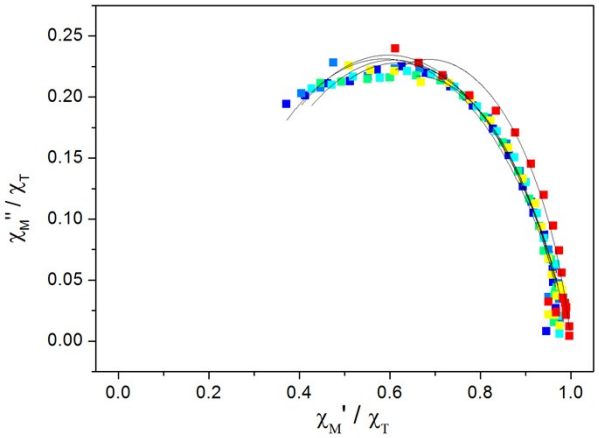

Figure S7. Normalized Cole-Cole diagram measured from 1.5 to 5 K for **DyAZO** with $\mathbf{H_{dc} = 0\ Oe}$. The solid lines represent some of the best fits with an extended Debye model.

Table S6. Adiabatic (χ_S), isothermic (χ_T) susceptibilities and relaxation times distribution (α) extracted for **DyAZO** with $\mathbf{H_{dc} = 0\ Oe}$.

T (K)	χ_S	χ_T	α	R^2
1.5	2.97	17.12	0.35	0.98496
1.6	2.76	16.92	0.36	0.99045
1.7	1.98	15.80	0.38	0.98711
1.8	2.46	14.75	0.36	0.99275
1.9	2.71	13.61	0.32	0.98594
2.0	2.46	12.84	0.33	0.98665
2.1	2.13	12.36	0.36	0.99242
2.2	2.43	11.57	0.32	0.98119
2.3	3.42	10.92	0.26	0.99683
2.4	2.13	10.54	0.33	0.98952
2.5	2.14	10.01	0.32	0.97908
2.6	1.89	9.69	0.35	0.99271
2.7	1.93	9.26	0.33	0.99245
2.8	1.78	8.93	0.34	0.99044
2.9	1.84	8.56	0.32	0.99287
3.0	1.74	8.28	0.33	0.98729
3.2	2.53	7.64	0.28	0.99952
3.4	1.64	7.22	0.31	0.98957
3.6	1.61	6.78	0.31	0.99004
3.8	1.52	6.42	0.31	0.9888
4.0	1.43	6.11	0.33	0.98681
4.2	1.43	5.82	0.31	0.98936
4.4	1.43	5.53	0.30	0.99128
4.6	1.5228	5.28	0.27	0.98913
4.8	1.5340	5.04	0.25	0.98551

5.0	1.7611	4.71	0.19	0.98515
5.2	1.6309	4.58	0.28	0.98738
5.4	1.6319	4.39	0.19	0.98804
5.6	1.467	4.10	0.18	0.9922
5.8	1.3480	3.98	0.19	0.9867

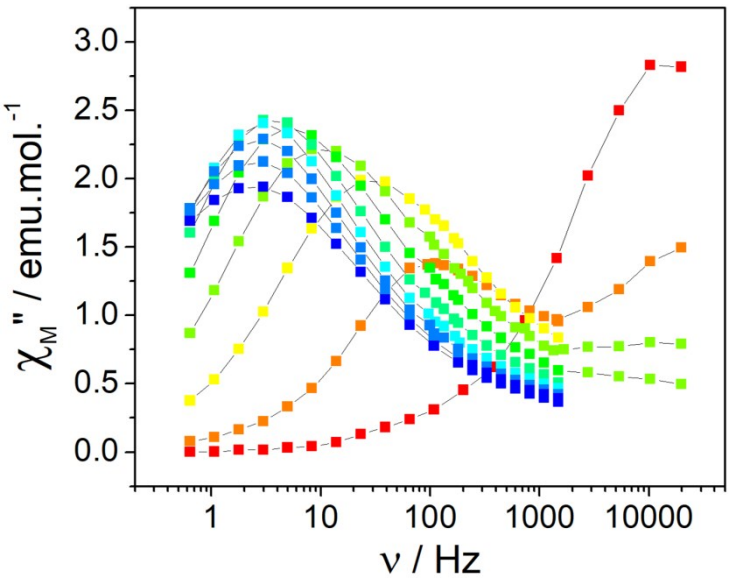

Figure S8. Frequency dependence of the out-of-phase component of the magnetization measured on **DyAZO** at 2 K, with H_{dc} between 0 Oe (red) and 1800 Oe (blue), 200 Oe spacing.

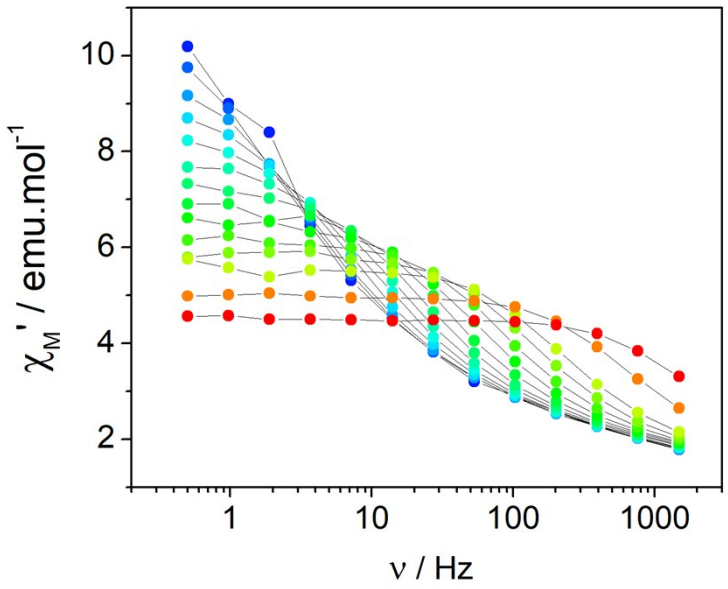

Figure S9. Frequency dependence of the in-phase component of the magnetization measured on **DyAZO** with **H_{dc} = 1200 Oe** between 2 K (blue) and 5 K (red) (0.2 K spacing between 2 K - 4 K and 0.5 K spacing between 4 K - 5 K).

Table S7. Relaxation times extracted for **DyAZO** with $\mathbf{H_{dc}}$ **= 1200 Oe**.

T (K)	τ (μs)	T (K)	τ (μs)
1.8	82900	2.9	8411
1.9	66270	3	6375
2	54698	3.1	5299
2.1	44993	3.2	4486
2.2	39117	3.4	2620
2.3	30000	3.6	1737
2.4	24115	3.8	1140
2.5	17903	4	691
2.6	15830		
2.7	12475		
2.8	10127		

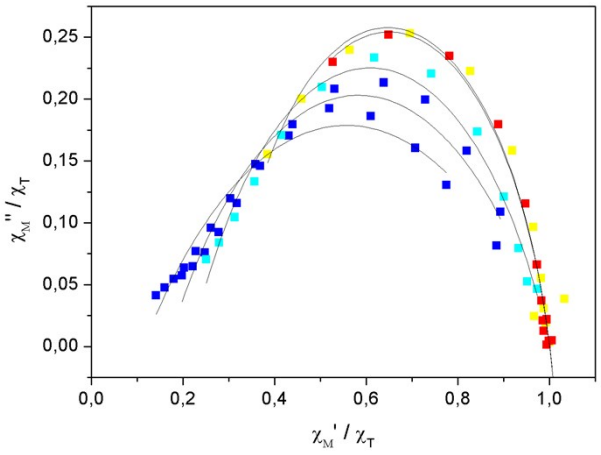

Figure S10. Normalized Cole-Cole diagram measured from 2 to 4.5 K for **DyAZO** with $\mathbf{H_{dc}}$ **= 1200 Oe**. The solid lines represent some of the best fits with an extended Debye model.

Table S8. Adiabatic (χ_S), isothermic (χ_T) susceptibilities and relaxation times distribution (α) extracted for **DyAZO** with $\mathbf{H_{dc}}$ **= 1200 Oe**.

T (K)	χ_S	χ_T	α	R^2
2.0	1.42	12.57	0.51	0.96459
2.5	1.53	9.19	0.41	0.92064
3.0	1.60	7.53	0.33	0.95907
4.0	1.63	5.56	0.19	0.93946
4.5	1.49	5.015	0.20	0.98069

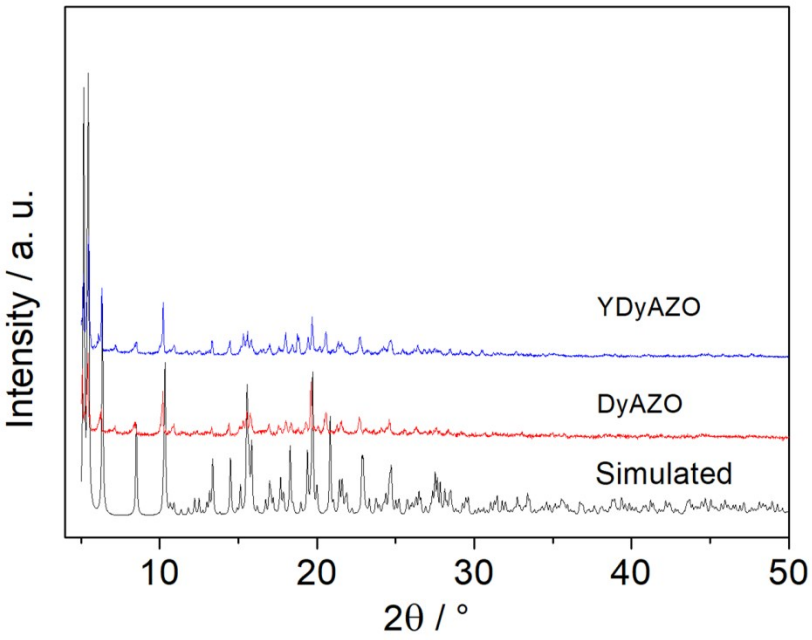

Figure S11. Powder X-ray diffraction patterns of microcrystalline powders of **DyAZO** and **YDyAZO** (measured at room-temperature) with comparison to the structural data file of **DyAZO** (at 150 K).

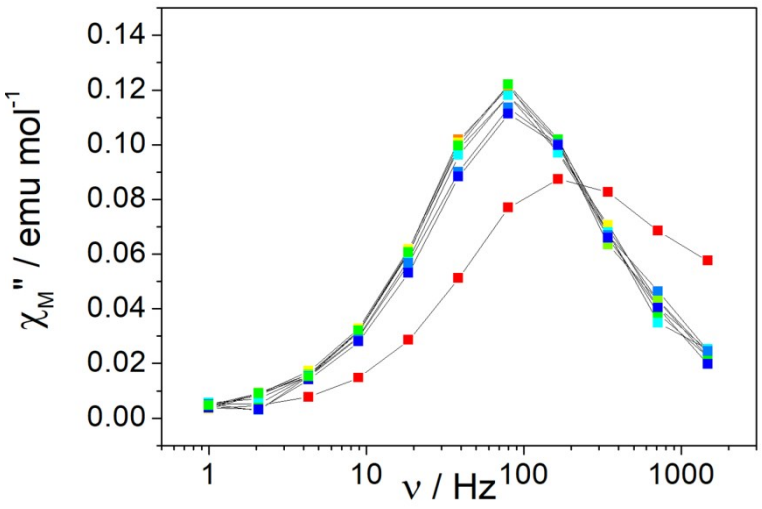

Figure S12. Frequency dependence of the out-of-phase component of the magnetization measured on **YDyAZO** at T = 4K, with H_{dc} between 0 Oe (red) and 1800 Oe (blue), 400 Oe spacing.

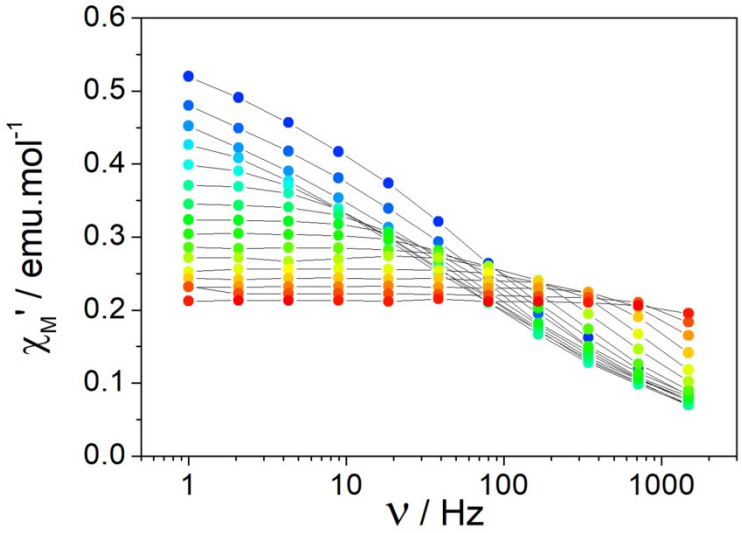

Figure S13. Frequency dependence of the in-phase component of the magnetization measured on **YDyAZO** with $\mathbf{H_{dc}}$**=0 Oe** between 2 K (blue) and 5.75 K (red) (0.25 K spacing)

Table S9. Relaxation times extracted for **YDyAZO** with $\mathbf{H_{dc}}$ **= 0 Oe**.

T (K)	τ (μs)	T (K)	τ (μs)
1.8	4191	3.5	1674
1.9	4076	3.8	1089
2	4027	4	709
2.3	3730	4.2	423
2.8	3301	4.5	299
3.2	2808	4.7	184

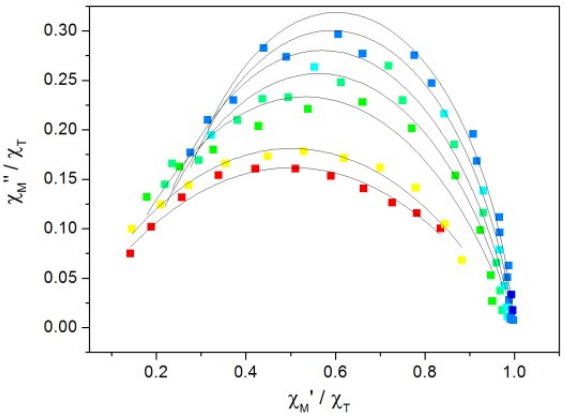

Figure S14. Normalized Cole-Cole diagram measured from 1.9 to 4.2 K for **YDyAZO** with $\mathbf{H_{dc}}$ **= 0 Oe**. The solid lines represent some of the best fits with an extended Debye model.

Table S10. Adiabatic (χ_S), isothermic (χ_T) susceptibilities and relaxation times distribution (α) extracted for **YDyAZO** with $\mathbf{H_{dc}}$ **= 0 Oe**.

T (K)	χ_S	χ_T	α	R^2
2.3	0.002	0.574	0.59	0.95736
2.8	0.001	0.483	0.55	0.9578
3.2	0.0253	0.389	0.41	0.90375
3.5	0.043	0.354	0.32	0.93394
3.8	0.046	0.328	0.26	0.94235
4.0	0.055	0.306	0.19	0.97783
4.2	0.058	0.286	0.14	0.98118

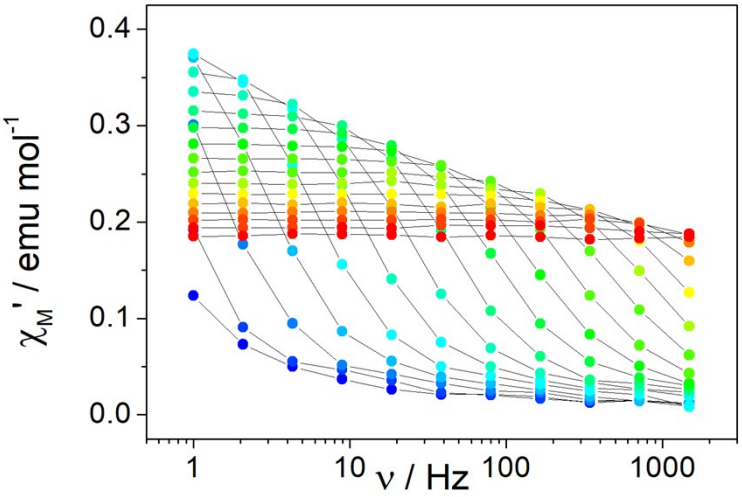

Figure S15. Frequency dependence of the in-phase component of the magnetization measured on **YDyAZO** with H_{dc} =1200 Oe between 2 K (blue) and 5.75 K (red) (0.25 K spacing)

Table S11. Relaxation times extracted for **YDyAZO** with $\mathbf{H_{dc}}$ **= 1200 Oe**.

T (K)	τ (μs)	T (K)	τ (μs)
2.8	54438	4	1895
3	25684	4.2	1023
3.2	12615	4.5	578
3.5	6529	4.8	323
3.8	3427	5	197

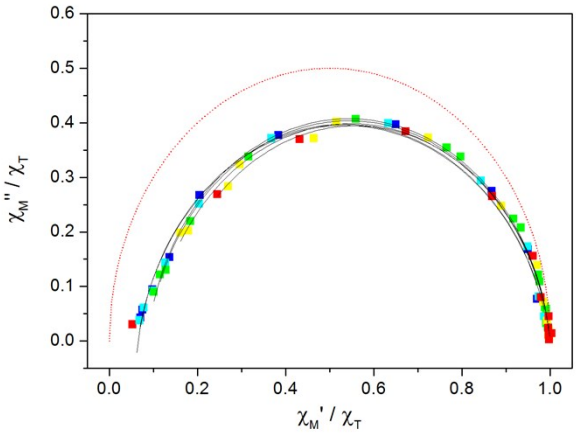

Figure S16. Normalized Cole-Cole diagram measured from 1.9 to 4.2 K for **YDyAZO** with **H_{dc} = 1200 Oe**. The solid lines represent some of the best fits with an extended Debye model. Dotted red line represents the ideal relaxation curve ($\chi_S/\chi_T = 0$, $\alpha = 0$).

Table S12. Adiabatic (χ_S), isothermic (χ_T) susceptibilities and relaxation times distribution (α) extracted for **YDyAZO** with **H_{dc} = 1200 Oe**.

T (K)	χ_S	χ_T	α	R^2
3.5	0.022	0.339	0.106	0.9798
4.0	0.025	0.298	0.072	0.99007
4.2	0.024	0.281	0.077	0.99159
4.5	0.025	0.266	0.079	0.98812
4.7	0.029	0.252	0.071	0.99157

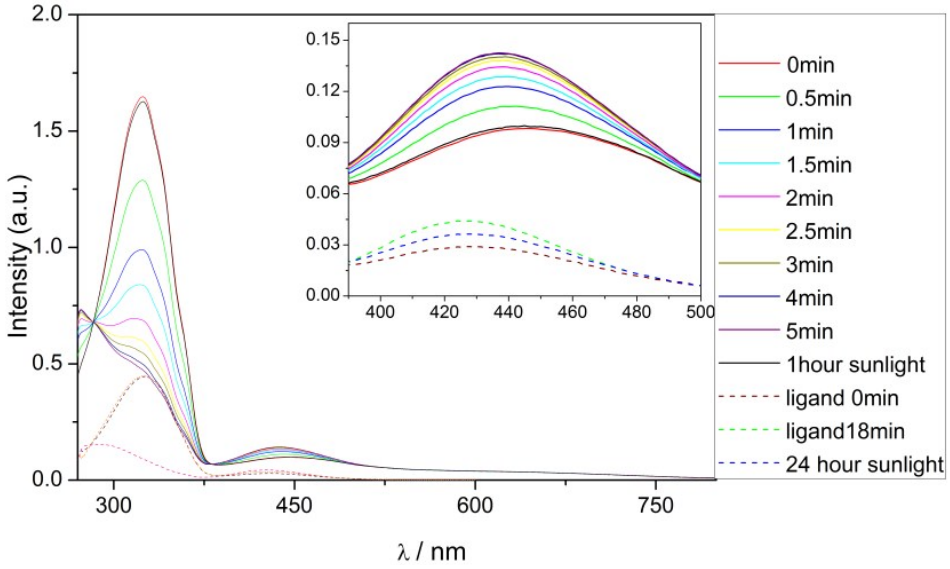

Figure S17. UV/Vis absorption spectra of a 1,4-dioxane solution (1 x 10^{-5} mol.L^{-1}) of **DyAZO** (full lines) and **AZO** (dotted lines) upon irradiation with UV (λ_{exc} = 365 nm, E_e = 2.40 mW.cm^{-2}).

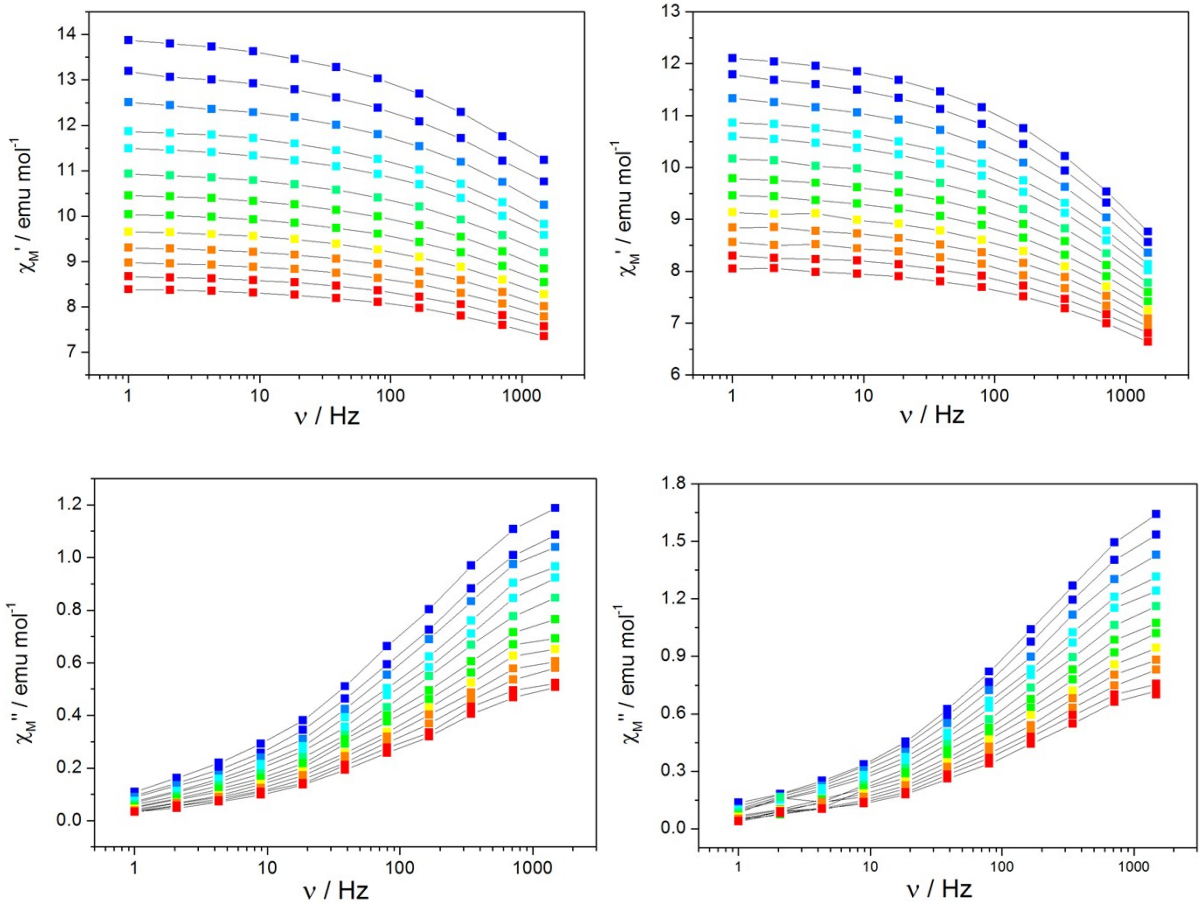

Figure S18. Frequency dependence of the in-phase and out-of-phase component of the magnetization measured on a 1,4-dioxane solution of *trans*-**DyAZO** with H_{dc} = 0 Oe (left) and H_{dc} = 1200 Oe (right) between 1.8 K (blue) and 3 K (red) (0.1 K spacing).

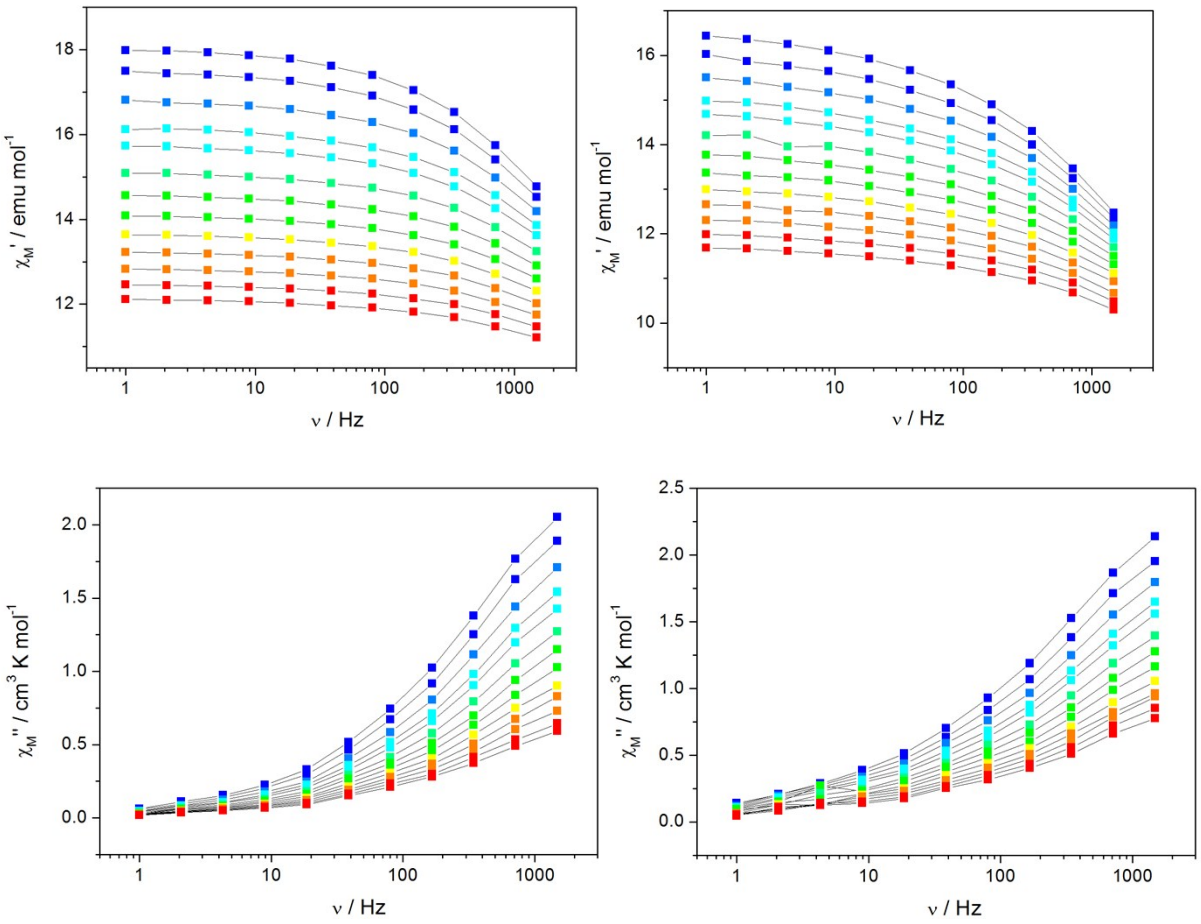

Figure S19. Frequency dependence of the in-phase and out-of-phase component of the magnetization measured on a 1,4-dioxane solution of *cis*-**DyAZO** with $H_{dc} = 0$ Oe (left) and $H_{dc} = 1200$ Oe (right) between 1.8 K (blue) and 3 K (red) (0.1 K spacing).

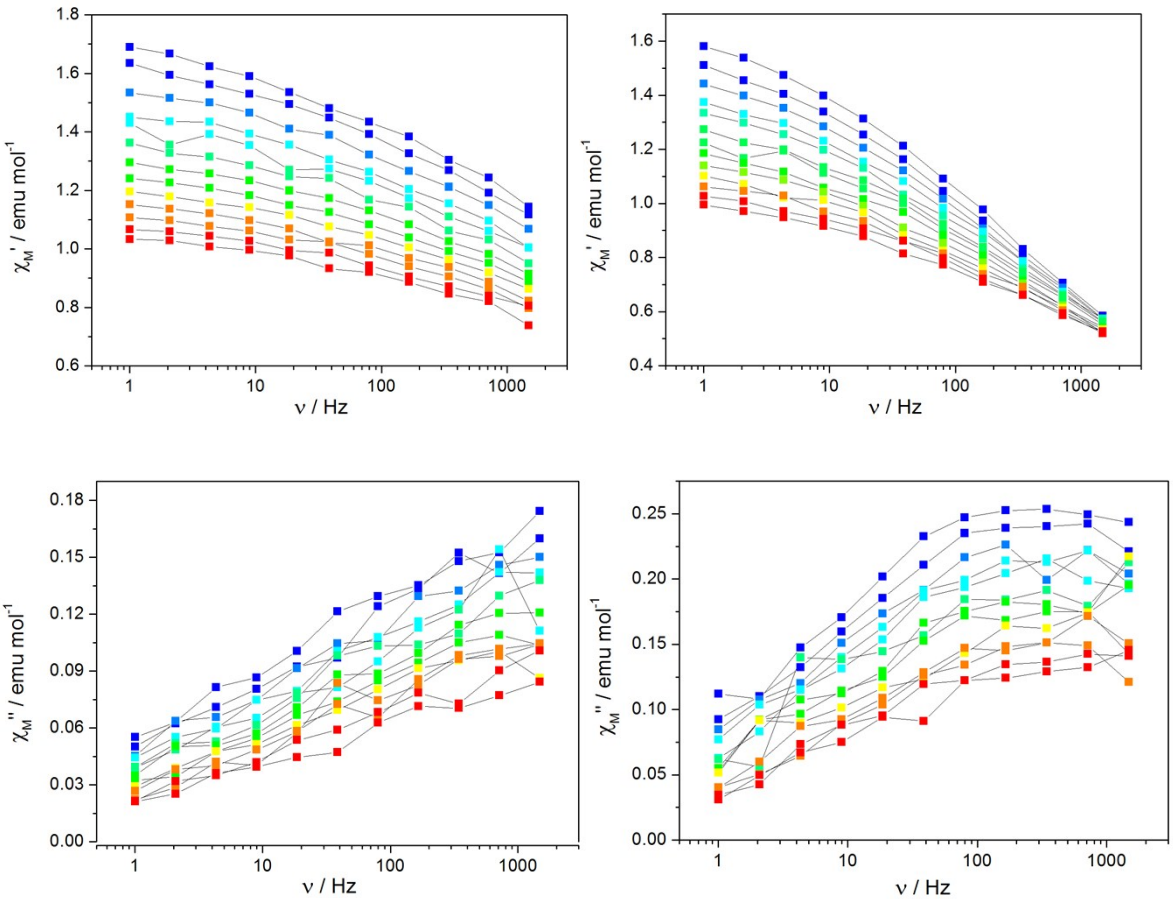

Figure S20. Frequency dependence of the in-phase and out-of-phase component of the magnetization measured on a 1,4-dioxane solution of *trans*-**YDyAZO** with H_{dc} =0 Oe (left) and H_{dc} = 1200 Oe (right) between 1.8 K (blue) and 3 K (red) (0.1 K spacing).

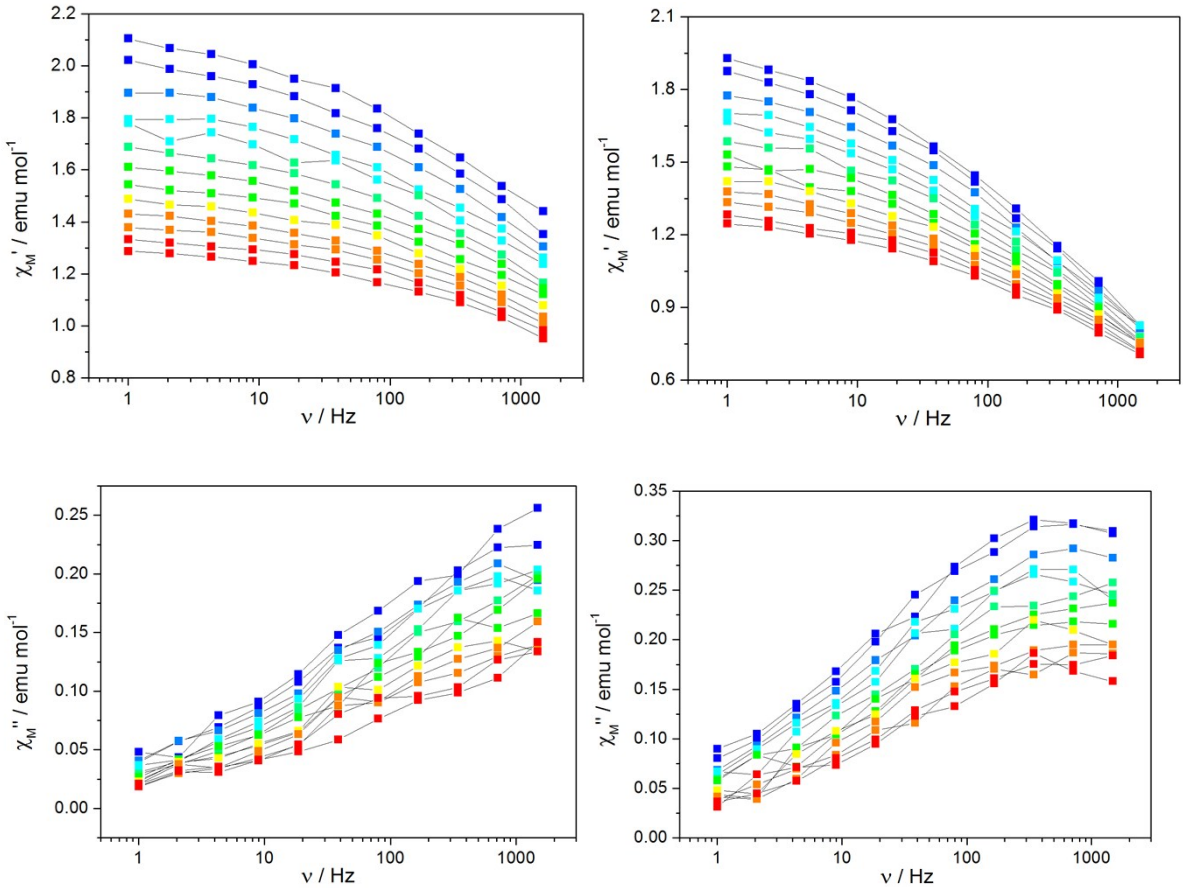

Figure S21. Frequency dependence of the in-phase and out-of-phase component of the magnetization measured on a 1,4-dioxane solution of *cis*-**YDyAZO** with $H_{dc} = 0$ Oe (left) and $H_{dc} = 1200$ Oe (right) between 1.8 K (blue) and 3 K (red) (0.1 K spacing).